THE ANALYST
FULL PAPER
www.rsc.org/analyst

Overoxidation of carbon-fiber microelectrodes enhances dopamine adsorption and increases sensitivity†

Michael L. A. V. Heien, Paul E. M. Phillips, Garret D. Stuber, Andrew T. Seipel and R. Mark Wightman*

Department of Chemistry and Neuroscience Center, Chapel Hill, NC 27599, USA. E-mail: rmw@unc.edu; Fax: +1 919 962 2388; Tel: +1 919 962 1472

Received 19th June 2003, Accepted 20th October 2003
First published as an Advance Article on the web 11th November 2003

The voltammetric responses of carbon-fiber microelectrodes with a 1.0 V and a 1.4 V anodic limit were compared in this study. Fast-scan cyclic voltammetry was used to characterize the response to dopamine and several other neurochemicals. An increase in the adsorption properties of the carbon fiber leads to an increase in sensitivity of 9 fold *in vivo*. However the temporal response of the sensor is slower with the more positive anodic limit. Increased electron transfer kinetics also causes a decrease in the relative sensitivity for dopamine *vs.* other neurochemicals, and a change in their cyclic voltammograms. Stimulated release in the caudate-putamen was pharmacologically characterized *in vivo* using Ro-04-1284 and pargyline, and was consistent with that expected for dopamine.

Introduction

An ideal sensor for the detection of neurotransmitters in the extracellular fluid of the brain has high sensitivity, can distinguish between compounds, and has a fast response time. Electrochemical approaches offer a way to accomplish this for easily oxidized neurotransmitters by using an electrode next to sites where the neurotransmitter is released. Dopamine is one candidate for detection in this way. It has receptor binding affinities ranging from nanomolar to micromolar[1,2] and thus low detection limits are required to monitor it in physiologically relevant situations. Since many other electroactive species are present in much higher concentrations, chemical selectivity is necessary to distinguish between them. Furthermore, because dopamine conveys information on a subsecond time scale, fast temporal response is needed to follow these changes.

Many strategies have been used to make dopamine detection with carbon-fiber microelectrodes approach these ideal properties. Rapid detection coupled to analyte identification has been accomplished with fast-scan cyclic voltammetry.[3] In this technique, cyclic voltammograms are repeated at regular intervals, typically 100 ms, to give subsecond time resolution. Each background-subtracted cyclic voltammogram provides information on the species detected while the amplitude of the dopamine oxidation current provides a measure of its instantaneous concentration. Thus, in contrast with amperometric or pulsed techniques, improved chemical identification is possible with cyclic voltammetry.[4] Further selectivity has been obtained by coating the electrode with a polymer. For example, Nafion®, a perfluorosulfonated ion exchange polymer, can exclude electroactive anions such as 3,4-dihydroxyphenylacetic acid (DOPAC) and ascorbic acid, while preconcentrating cations such as dopamine at the electrode surface.[5] Overoxidized polypyrrole exhibits similar properties.[6,7] However, with both polymers, a slower response time is also observed.

The sensitivity of fast scan cyclic voltammetry for dopamine can be increased by electrochemical treatments. Indeed, the first paper on the electroanalytical use of carbon electrodes by Lord and Rogers showed that anodization of graphite caused a higher limiting current for the reduction of ferric ion.[8] Later, it was shown that sensitivity for dopamine could be increased at a carbon-fiber microelectrode by pretreatments that involved repetitive excursions to +3.0 V *vs.* Ag/AgCl at 70 Hz.[9,10] Such treatments dramatically change the surface properties as demonstrated by scanning electron microscopy (SEM)[11] and increase surface oxides. Another strategy is to scan the electrode continuously to an anodic potential. Presumably this also oxidizes the carbon surface.[12] Stamford and coworkers found a seven-fold increase in sensitivity to dopamine by scanning the potential to +1.4 V *vs.* Ag/AgCl during the waveform.[13] Brajter-Toth has reported increased sensitivity to adenosine and uric acid while scanning to +1.5 V *vs.* SCE.[14–16] A similar waveform was used for dopamine detection at electrodes coated with polypyrrole,[6,7] and increased sensitivity was demonstrated.

In this work we compare the cyclic voltammetric response of uncoated electrodes to dopamine when used with either 1.0 V or 1.4 V potential limit (*vs.* Ag/AgCl). Uncoated electrodes were used to minimize a decrease in response times. The extended limit significantly increases the sensitivity to dopamine and places it in the range necessary to detect dopamine changes during behavior.[17] In addition, we recorded the voltammograms of several neurochemicals with the extended waveform and evaluated it during *in vivo* use.

Experimental

Chemicals

Unless noted, all chemicals were purchased from Sigma-Aldrich (St. Louis, MO) and used as received. Ro 04-1284 was a gift from Hoffmann–La Roche (Nutley, NJ). Solutions were prepared using doubly distilled deionized water (Megapure system, Corning, New York). TRIS buffer solution, pH 7.4, (15 mM TRIS, 140 mM NaCl, 3.25 mM KCl, 1.2 mM $CaCl_2$, 1.25 mM NaH_2PO_4, 1.2 mM $MgCl_2$, 2.0 mM Na_2SO_4) was used in all flow injection analysis experiments. Stock solutions of analyte were prepared in 0.1 N $HClO_4$, and dilute solutions were made in TRIS buffer on the day of use.

† Electronic supplementary information (ESI) available: National Instruments Data Acquisition System. See http://www.rsc.org/suppdata/an/b3/b307024g/

Electrodes

Glass-encased carbon fiber T-650 (Thornel, Amoco Corp., Greenville, SC) microelectrodes were constructed as previously described.[18] Individual carbon fibers were aspirated into glass capillaries (A-M Systems, Carlsborg, WA) and the glass was tapered with a micropipette puller (Narashige, Tokyo, Japan). The carbon fiber was then sealed in the capillary with epoxy (Epon 828 with 14% *m*-phenylenediamine by weight, Miller-Stephenson Chemical Co., Danbury, CT), excess epoxy was removed with acetone, and the assembly was cured (100 °C for 12 h, 150 °C for 2 days). The protruding carbon fiber was then cut to a length between 50 and 100 μm. On the day of use electrodes were soaked in isopropanol purified with Norit A activated carbon (ICN, Costa Mesa, CA) for at least 10 min,[19] then backfilled with electrolyte (4 M potassium acetate, 150 mM potassium chloride), and fitted with wires for electrical contact. The geometric area of the electrodes was calculated using the nominal radius of the carbon fibers, and the length. The length was measured using optical microscopy. A silver/silver chloride electrode served as the reference.

Data Acquisition

Cyclic voltammograms were acquired using data acquisition hardware and local software written in LabVIEW (National Instruments, Austin, TX). The program was a modification of that described previously.[20] The present version eliminates the use of the phase locked loop, and requires a low noise current amplifier. The timing board of the prior system was deleted and its functions were distributed between two boards (PCI-6052E and PCI-6711E, National Instruments). The cyclic voltammogram waveform was generated and the voltammetric signal was acquired with the PCI-6052E. The PCI-6711E was used to synchronize waveform application, data acquisition, stimulation delivery, and flow injection. For a detailed description of the data acquisition, see Electronic Supplementary Information (ESI)†. After collection, background subtraction, signal averaging, and digital filtering were all done under software control.

The computer generated waveform was filtered and attenuated four-fold before application to the electrode to reduce the staircase steps in the digitally generated waveform. The waveform was then input into a custom built instrument for application to the electrochemical cell and current transduction (UNC Department of Chemistry Electronics Shop). The output signal was low pass filtered at 50 kHz before being digitized.

Flow injection apparatus

The electrode was positioned at the outlet of a 6-port rotary valve. A loop injector was mounted on an actuator (Rheodyne Model 5041 valve and 5701 actuator) which was used with a 12 V DC solenoid valve kit (Rheodyne, Rohnert Park, CA) to introduce the analyte to the surface of the electrode.[21] Solvent flow (1.0 cm s^{-1}) was driven with a syringe infusion pump (Harvard Apparatus Model 22, Holliston, MA) through the valve and into the electrochemical cell. The response time of the electrode was measured as the amount of time required to rise from 10% to 90% of the maximum response of the injection.

Data analysis

Data analysis was performed with local software written in LabVIEW. With the scan rates employed, a large background current is generated that may be 100 times greater then the faradic current. The background current is stable and can be subtracted from the current in the presence of analyte, yielding a background-subtracted cyclic voltammogram. These are characteristic of the detected species. To obtain temporal information on changes in analyte concentration the current at the peak oxidation potential for dopamine for each cyclic voltammogram is plotted *vs*. time. This is converted to concentration with an electrode calibration. The apparent capacitance of the carbon-fiber microelectrode was calculated by measuring the current at −0.2 V, and dividing by the scan rate applied and the geometric area of the microelectrode. Cyclic voltammogram simulations were generated with Digi-Sim (Bioanalytical Systems Inc., West Lafayette, IN).

Biological experiments

For *in vivo* experiments, male Sprague-Dawley rats (250–400 g; Charles River Laboratories, Wilmington, MA) were anesthetized with 50% w/w urethane in saline solution (0.3 mL per 100 g rat weight) and mounted in a stereotaxic frame (Kopf Instruments, Tujunga, CA). Holes were drilled in the skull to allow access to the caudate-putamen for microelectrode placement (stereotaxic coordinates from bregma: 1.2 mm anterior; 2.0 mm lateral; 4.5 mm ventral) and to the substantia niagra/ventral tegmental area (SN/VTA) for stimulator placement (stereotaxic coordinates from bregma: 5.6 mm posterior; 1.0 mm lateral; 7.5 mm ventral).[22] Body temperature was maintained at 37 °C with a constant temperature heating pad (Braintree, Braintree, MA). A twisted bipolar stimulating electrode (Plastics One, Wallingford, CT) provided constant-current, stimulation pulses to the SN/VTA. To avoid electrical crosstalk, the stimulation did not occur during individual cyclic voltammograms, but during the rest period between them. The stimulus was also optically isolated from the signal generation apparatus (NeuroLog System, Hertfordshire, England). A 60 pulse, 60 Hz biphasic (±125 μA, 2 ms per phase) stimulation was used for all *in vivo* experiments. There was a 2 ms delay between the end of the stimulus and the beginning of the next cyclic voltammogram.

Results and discussion

Electrochemical treatment

Previously for the detection of dopamine, we used a triangular waveform from an initial potential of −0.4 V to 1.0 V *vs*. Ag/AgCl, and back to −0.4 V at 300 V s^{-1}.[18] Between voltammograms the potential was held at −0.4 V. The triangular waveform was repeated at a frequency of 10 Hz. This waveform has previously been characterized, and it was shown that sensitivity approached a maximum at this repetition rate.[19] This scan protocol will be referred to as the "traditional waveform." The background current with the traditional waveform due to charging of the double layer and oxidation of surface oxide groups[23] is shown in Fig. 1 (Panel A, dashed line). A background-subtracted cyclic voltammogram for 1 μM dopamine obtained with this waveform is shown in Panel B. The temporal response to a bolus of dopamine is shown in Panel C; the current at the oxidation potential for dopamine is plotted *vs*. time. The response time of electrodes under these scan parameters is 0.6 s. Panel D shows a calibration curve for dopamine; the response is linear for the biologically relevant concentrations shown.

We have previously shown that the signal for dopamine with the traditional waveform arises from its adsorption to the carbon fiber surface.[19] The amplitude of the signal is larger than expected for purely diffusion-controlled processes, because dopamine accumulates on the electrode between voltammetric scans. This preconcentration lowers detection limits; however, it slows the response time of the electrode to concentration

changes. In this work we found that the degree of adsorption is a function of the rest potential. With the anodic limit kept constant at 1.0 V, the holding potential was varied from 0.0 V to −0.8 V. As the holding potential is made more negative, an increase in signal is seen (Fig. 2, Panel A, open bars), presumably due to increased electrostatic interactions of the cation dopamine with the negatively-charged electrode surface.

By increasing the anodic potential limit during a scan from 1.0 V, to 1.4 V, increased sensitivity to dopamine was observed. We chose this potential limit, because at potentials more positive than 1.4 V, a large background peak is observed at the switching potential (data not shown). The holding potential was varied in the same manner as described above and the signal for dopamine was monitored (Fig. 2, Panel A, shaded bars). Again, as the holding potential is made more negative, an increase in signal is seen. The scans with the more positive anodic limit show a greater dependence on the resting potential. For both scan ranges the error is greatest with the most negative potential. This may be due to electrolysis of solvent at the holding potential.[15]

Extended Waveform

We investigated the waveform with potential limits of −0.6 V and 1.4 V in more detail; a scan rate of 400 V s^{-1} was used so that it was of approximately the same duration as the traditional waveform. The shorter duration allowed the stimulus pulses to fit between cyclic voltammograms. This waveform is referred to as the "extended waveform." The background current is in Fig. 1, Panel A, solid lines. The background current is approximately twice as large as with the traditional waveform, with the apparent capacitance of the electrode increasing from 26 μF cm^{-2} to 49 μF cm^{-2}. The cyclic voltammogram for 1 μM dopamine with this waveform is shown in Panel B. The voltammogram shows a significant increase in the oxidation current for dopamine (solid line *vs*. dashed line). In Panel C the current at the peak oxidation potential for dopamine is plotted *vs*. time for a square bolus of dopamine. The increase in sensitivity is clearly apparent; however the response time with the extended waveform is decreased to 1.2 s. Slower temporal responses have been previously reported with electrochemically pretreated carbon electrodes.[24] A calibration curve is located in Panel D. The increase in sensitivity over the traditional waveform is 4.9, and the increase in signal to noise is 4.0. This increase leads to limits of detection (3 times standard deviation of the noise) of less than 5 nM. This increase makes the use of this waveform attractive for situations requiring detection of low concentrations of dopamine. The response is linear over the range shown; but deviates from linearity at concentration above 5 μM.

The increase in sensitivity could be due to an increase in microscopic surface area or a change in the chemical structure of the electrode surface. Because the background current is proportional to the electrode area, if the increase in signal were solely due to an increase in electrode area, the increase in sensitivity would be expected to be similar, ~2-fold. Since a larger increase in signal is seen, it suggests that the increase in adsorption is due to more sites available for adsorption per unit area. Indeed, no changes in the electrode surface were seen at relatively high magnification (×10,000) when examined by SEM (data not shown).

Part of the increase in signal can be attributed to an increase in scan rate. The remainder must be due to increased surface area, and increased adsorption. Therefore to test whether this gain in sensitivity was a result of increased capacity for dopamine to adsorb to the carbon-fiber microelectrodes, adsorption isotherms were constructed for dopamine using both waveforms. Isotherms for the traditional waveform have been previously reported,[19] and an isotherm for the extended waveform is shown in Fig. 2. In this experiment, the dopamine concentration was varied from 1 μM to 500 μM and the peak oxidation current was plotted *vs*. concentration (Panel B, open circles). The peak current has two contributors: adsorption and diffusion. The dashed line is the diffusion-controlled current obtained by simulation of the experimental conditions. This was subtracted from the experimental data to yield the adsorption component alone. By integrating the area under the oxidation peak, one can measure the amount of adsorbed dopamine leading to the isotherm (Fig. 2, Panel C). The data was fit to the equation for a Langmuir isotherm:

$$\frac{\Gamma_{DA}}{\Gamma_S - \Gamma_{DA}} = \beta[DA] \quad (1)$$

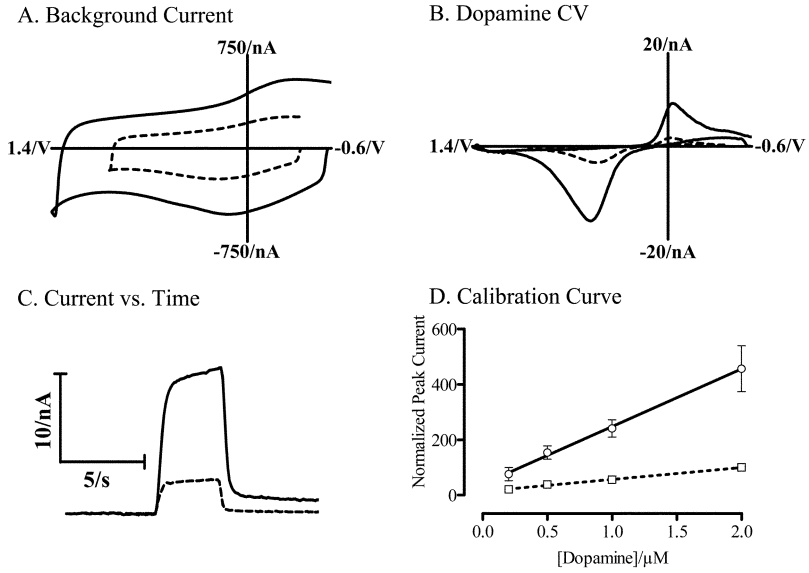

Fig. 1 *In vitro* characterization of waveforms. The traditional waveform (−0.4 V to 1.0 V, 300 V s^{-1}) is shown in dashed lines, while the extended waveform (−0.6 V to 1.4 V, 400 V s^{-1}) is shown in solid lines. A: Background cyclic voltammograms for the two potential limits at the same electrode recorded in TRIS buffer solution, pH 7.4. B: Background-subtracted cyclic voltammograms for 1 μM dopamine. C: Response to a bolus dopamine injection, in which the peak oxidation current of each cyclic voltammogram is plotted *vs*. time. D: Calibration curve for dopamine (n = 6). Due to variations between electrodes, each electrode response was normalized to the response for 2 μM dopamine with the traditional waveform. The error bars represent the standard deviation.

where Γ_{DA} is the surface concentration of dopamine, Γ_S is the saturation coverage, and β is the equilibrium constant for adsorption. At low dopamine concentrations, the surface coverage will be small when compared to the saturation coverage, and a linearized form of the isotherm is obtained:

$$\Gamma_{DA} = b[DA] \quad (2)$$

where $b = \Gamma_s\beta$. For the traditional waveform Γ_S = 41 pmol cm^{-2}, $\beta = 2.5 \times 10^{-5}$ cm^3 pmol^{-1}, yielding $b = 1.0 \times 10^{-3}$ cm. The adsorption isotherm for the extended waveform (Fig. 2, Panel C) cannot be fit to eqn. (1) alone. Instead an isotherm with Γ_S = 92 pmol cm^{-2}, $\beta = 6.9 \times 10^{-5}$ cm^3 pmol^{-1}, yielding $b = 6.4 \times 10^{-3}$ cm plus a linear component having a slope of 0.9×10^{-3} cm were fit to the data. Note that the overoxidation doubles both the saturation coverage and the apparent capacitance.

The electrode's temporal response to dopamine is related to the amount of adsorption. In Fig. 1, panel C, the response to dopamine does not return to baseline immediately. This is true for both the traditional waveform and the extended waveform. However, the adsorption is reversible, and the signal does return to baseline after approximately a minute, making successive measurements possible.

Selectivity

High sensitivity is not the only desirable factor when choosing a sensor. Selectivity between analytes is also required. This is especially important in the brain where many molecules can interfere with the analyte of interest. Fig. 3 shows the background-subtracted cyclic voltammograms for various neurotransmitters, their metabolites, and other biologically active substances. The dashed lines are for voltammograms obtained with the traditional waveform, while the solid lines were obtained with the extended waveform. In the brain, dopamine is metabolized by monoamine oxidase (MAO) to form DOPAC. Panel A shows the cyclic voltammogram for dopamine, while panel B shows DOPAC. With the traditional waveform the slow electron transfer kinetics for DOPAC distinguish it from dopamine. However, with the extended waveform the peaks for DOPAC become sharper because of faster kinetics, and the oxidation peak overlaps that for dopamine. DOPAC can be further metabolized by catechol-*o*-methyltransferase (COMT) to form homovanillic acid (HVA), whose voltammogram is in Panel D. Using traditional scan parameters there is no current due to the oxidation of HVA, while the use of the extended waveform voltammogram reveals both oxidation and reduction peaks. Dopamine can also be metabolized by COMT to form 4-hydroxy-3methoxyphenylethylamine (3-MT), whose voltammogram is in Panel C. The voltammograms can be easily distinguished from dopamine.

Panel E and F of Fig. 3 show the voltammograms for another neurotransmitter, serotonin, and its metabolite 5-hydoxyindole acetic acid. The voltammograms with both the traditional waveform and the extended waveform are distinguishable from dopamine. Sharper peaks and increased sensitivity are also observed for these analytes with the extended waveform. The voltammogram for norepinephrine (Panel G), another neurotransmitter, is very similar to that of dopamine with both waveforms.

Another *in vivo* interferent is a change in pH. The background at a microelectrode is pH dependent, because pH affects the protonation of surface oxides and alters double layer structure.[23] Because background subtraction makes fast scan cyclic voltammetry a differential technique, any species that changes the background current causes a signal. *In vivo* changes in pH occur and have been measured with fast-scan cyclic voltammetry following electrical stimulation of dopamine neurons.[25] Both the traditional and extended waveforms show similar amplitudes for changes in pH. Two more interferents, ascorbic acid, and uric acid are located in panels I and J respectively. The extended waveform gives a better defined oxidation wave for ascorbic acid. The traditional waveform shows no electrooxidation current for uric acid, whereas the extended waveform shows oxidation and reduction waves.

The identity of a particular analyte is determined by the oxidation potentials, and the shape of the oxidation wave. A correlation coefficient can be calculated for each voltammetric wave with relation to dopamine, as has been previously reported.[26,27] During an experiment, each voltammogram collected is compared to that of the desired analyte. The r^2 is then calculated, and is used to confirm the identity of the analyte. When compared to dopamine, the cyclic voltammograms using the extended waveform in Fig. 3 exhibit an r^2 with a value less than 0.85, with the exception of norepinephrine, which correlates highly with that for dopamine (r^2 = 0.98). This is in contrast to the traditional waveform, where the r^2 are less than 0.52, again, with the exception of norepinephrine (r^2 = 0.93). The correlation coefficients between dopamine and the compounds in Fig. 3 can be seen in Table 1. The table shows that selectivity for dopamine over interferents is decreased with the extended waveform.

Overall, when comparing the cyclic voltammograms obtained with the traditional and extended waveforms, two trends are observed. Increases in sensitivity and electron transfer kinetics are observed for the extended scan limits. This makes the voltammograms of several substances, especially DOPAC, more similar to dopamine. Thus, the selectivity for dopamine is not as good with the extended waveform. To improve this, the electrode can be coated with polypyrrole. It further increases the

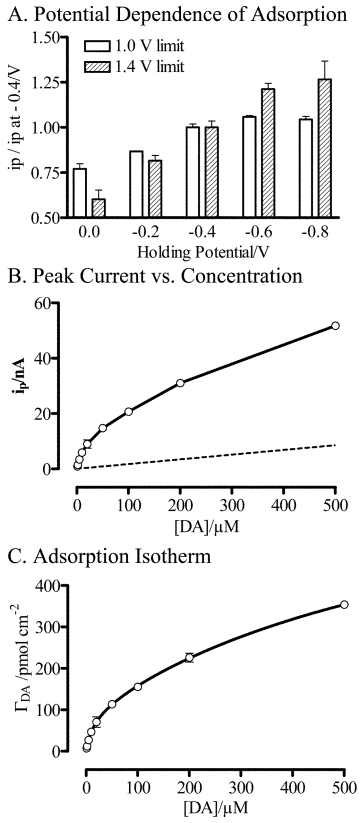

Fig. 2 Adsorption characteristics of dopamine. A: The effect of the holding potential on the peak current for dopamine. Values are normalized to the current with an initial potential of −0.4 volts. Open bars are for a 1.0 V anodic scan limit, and filled bars represent a 1.4 V anodic scan limit. B: Voltammetrically measured oxidative peak currents for dopamine as a function of dopamine concentration. The dashed line represents the simulated diffusion controlled responses. C: Fit of the diffusion corrected experimental data (circles) to a Langmuir isotherm with two components (solid line), the error bars represent the standard deviation.

sensitivity to dopamine, and excludes ascorbic acid and DOPAC.[7]

In vivo results

Because the extended waveform was less chemically selective, we wanted to test how this affected *in vivo* measurements. During these experiments, the working electrode was placed in a brain region where dopamine is released (caudate-putamen), and a stimulating electrode was placed near the dopamine cell bodies (SN/VTA). Electrical impulses delivered by the stimulating electrode produce action potentials in the dopaminergic neurons. When the action potentials reach the terminals, they cause dopamine release that can be detected with the carbon-fiber microelectrode. Each stimulation train evokes the release of a reproducible concentration of dopamine at a particular measurement location. Data collected *in vivo* is shown in Fig. 4, with the traditional waveform results shown with dashed lines, and the extended waveform results shown with solid lines. Panel A shows the background current observed, and Panel B shows the background-subtracted cyclic voltammogram for dopamine measured during and after stimulation of the dopamine neurons. The increase in sensitivity seen *in vivo* is larger than that measured *in vitro* (9 ± 2 fold *vs.* 4.9 ± 2). The background is similar to that seen *in vitro*, only an extra peak was seen around the oxidation potential for dopamine. This peak is observed in parts of the brain not containing dopamine, and is smaller when polypyrrole is present on the electrode (data not shown), suggesting its origin may be extracellular ascorbate.

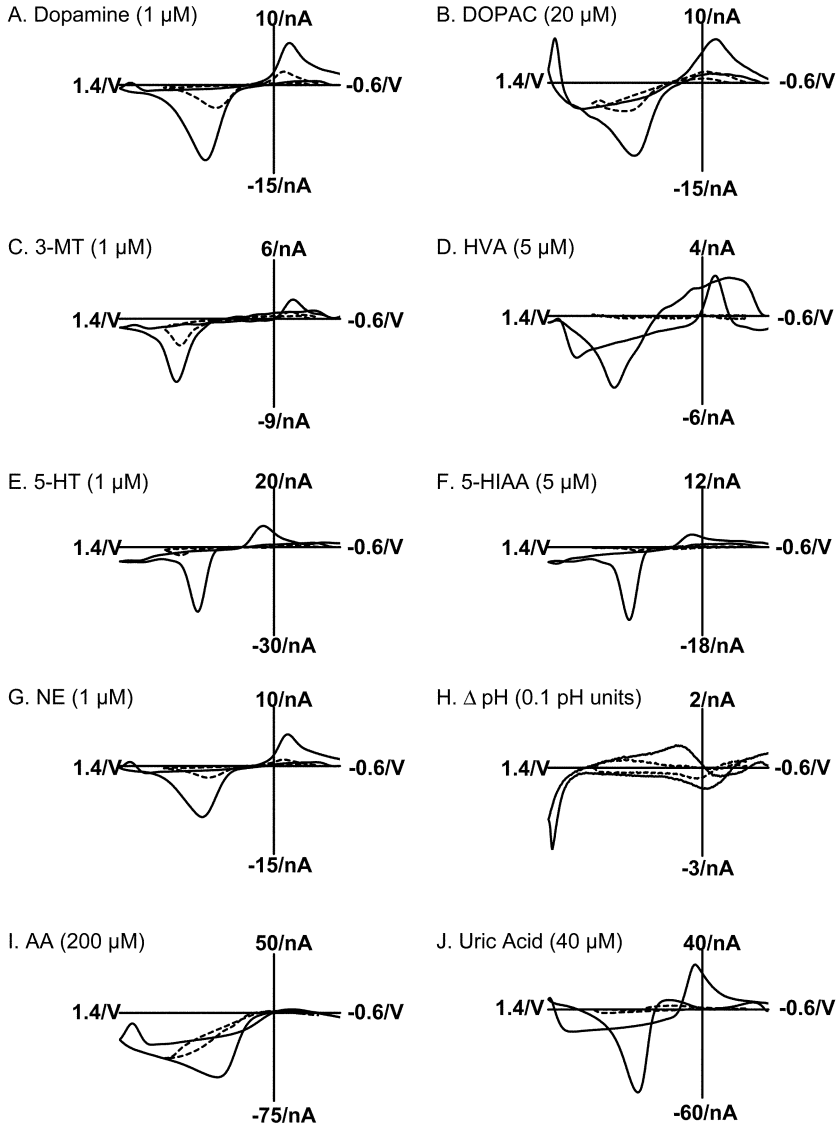

Fig. 3 The background-subtracted cyclic voltammograms for various compounds. Dashed lines show the voltammograms obtained using the traditional waveform, and the solid lines show the waveforms obtained with the extended waveform. The cyclic voltammograms were taken 300 ms after exposure to the analyte.

Table 1 Correlation coefficients between cyclic voltammograms for dopamine and for the various other neurochemicals in Fig. 3 (n = 3 electrodes, values are with standard deviations). Both values for the traditional and extended waveform are shown

	DOPAC	3-MT	HVA	5-HT	5-HIAA	NE	ΔpH	AA	Uric Acid
Traditional waveform	0.52 ± 0.04	0.28 ± 0.12	0.03 ± 0.03	0.20 ± 0.04	0.39 ± 0.17	0.90 ± 0.03	0.25 ± 0.05	0.23 ± 0.11	0.04 ± 0.03
Extended waveform	0.85 ± 0.10	0.43 ± 0.11	0.41 ± 0.07	0.63 ± 0.08	0.74 ± 0.06	0.95 ± 0.04	0.09 ± 0.05	0.65 ± 0.07	0.73 ± 0.06

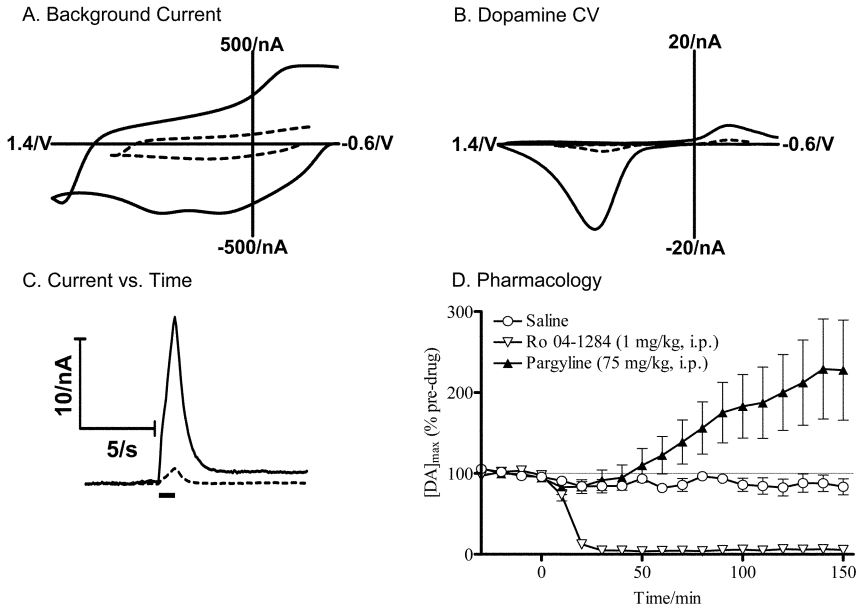

Fig. 4 *In vivo* characterization of waveforms. Results with the traditional waveform (−0.4 V to 1.0 V) are shown in dashed lines, while results with the extended waveform (−0.6 V to 1.4 V) are shown in solid lines. A: Background cyclic voltammograms for the two potential limits at the same electrode. B: Background-subtracted cyclic voltammograms obtained during a 60 pulse stimulation delivered at 60 Hz. C: Temporal response to the same stimulation obtained for oxidation current of each cyclic voltammogram. The solid bar represents the duration of the stimulation. D: Pharmacological responses of dopamine. Injections of either saline (open circles), pargyline (solid triangles), or Ro 04-1284 (open triangles) were given at time 0 (n = 4 rats). The error bars represent SEM.

Panel C is the current measured at the peak oxidation potential *vs.* time. The extended waveform has a slower response time, and this appears to slow further over the course of the experiment (data not shown). Thus, the extended waveform is not optimal when kinetic information concerning the signal is required.

However, the signal measured with these electrochemically treated electrodes is pharmacologically consistent with that expected for dopamine (Fig. 4, Panel D). Voltammetric release was monitored at 10 min intervals until a reproducible signal was measured. This sometimes required more than 1 h of measurements. After stable release during four consecutive measurements was obtained, either saline, pargyline, or Ro 04-1284 was administered. Two hours after administration, the amplitude of the evoked release in the saline treated animals was 83 ± 10% of the initial measurements. The drug pargyline inhibits the MAO catalyzed conversion of dopamine to DOPAC.[28,29] Following its administration, stimulated release did not decrease, indicating that DOPAC was not responsible for the measured signal. Rather it increased to 230 ± 60% of the baseline, consistent with more dopamine being available for packaging into vesicles and released when MAO is inhibited. Another drug, Ro 04-1284 was administered that inhibits the vesicular monoamine transporter, the protein responsible for packaging monoamines into vesicles for release.[30,31] If the measured signal is of dopamine origin, the drug should decrease the observed concentration. In fact, stimulated release almost completely vanished, decreasing to 5 ± 4% of baseline.

Conclusions

This report has characterized the cyclic voltammetric response of uncoated carbon-fiber microelectrodes to dopamine when used with a 1.0 V and a 1.4 V potential limit (*vs.* Ag/AgCl). Overoxidation doubles both the apparent capacitance and the saturation coverage for dopamine. The increase in sensitivity comes at the expense of temporal response. The 1.4 V potential limit alters the electron transfer kinetics at the electrode, causing a decrease in the selectivity for dopamine over the other compounds studied. However, this can be circumvented by independent signal characterization. Indeed, pharmacological characterization of the electrically evoked signal *in vivo* demonstrated consistency with dopamine. Importantly, this treatment causes an increase in the sensitivity of carbon fiber electrodes by changing the adsorption properties of the electrode allowing lower limits of dopamine detection (< 5 nM) to be obtained. The potential limits used are important, and other limits might be optimal.

Acknowledgement

The authors thank Heidi B. Martin for technical assistance and Regina Carelli for helpful discussions. This work was financed by NIH (NS15841).

References

1 J. D. Berke and S. E. Hyman, *Neuron*, 2000, **25**, 515.
2 E. K. Richfield, J. B. Penney and A. B. Young, *Neuroscience*, 1989, **30**, 767.
3 J. O. Howell, W. G. Kuhr, R. E. Ensman and R. M. Wightman, *J. Electroanal. Chem.*, 1986, **209**, 77.
4 J. E. Baur, E. W. Kristensen, L. J. May, D. J. Wiedemann and R. M. Wightman, *Anal. Chem.*, 1988, **60**, 1268.
5 G. A. Gerhardt, A. F. Oke, G. Nagy, B. Moghaddam and R. N. Adams, *Brain Res.*, 1984, **290**, 390.
6 C. C. Hsueh and A. Brajter-Toth, *Anal. Chem.*, 1994, **66**, 2458.
7 K. Pihel, Q. D. Walker and R. M. Wightman, *Anal. Chem.*, 1996, **68**, 2084.
8 S. S. Lord and L. B. Rogers, *Anal.Chem.*, 1954, **26**, 284.
9 F. Gonon, M. Buda, R. Cespuglio, M. Jouvet and J. F. Pujol, *Nature*, 1980, **286**, 902.
10 F. G. Gonon, C. M. Fombarlet, M. J. Buda and J. F. Pujol, *Anal. Chem.*, 1981, **53**, 1386.
11 G. M. Swain and T. Kuwana, *Anal. Chem.*, 1991, **63**, 517.
12 Y. W. Alsmeyer and R. L. McCreery, *Langmuir*, 1991, **7**, 2370.

13 S. Hafizi, Z. L. Kruk and J. A. Stamford, *J. Neurosci. Methods*, 1990, **33**, 41.
14 R. Bravo, C. C. Hsueh, A. Jaramillo and A. Brajter-Toth, *Analyst*, 1998, **123**, 1625.
15 R. Bravo and A. Brajter-Toth, *Chem. Anal. (Warsaw)*, 1999, **44**, 423.
16 A. Brajter-Toth, K. A. el Nour, E. T. Cavalheiro and R. Bravo, *Anal. Chem.*, 2000, **72**, 1576.
17 P. E. Phillips, G. D. Stuber, M. L. Heien, R. M. Wightman and R. M. Carelli, *Nature*, 2003, **422**, 614.
18 K. T. Kawagoe, J. B. Zimmerman and R. M. Wightman, *J. Neurosci. Methods*, 1993, **48**, 225.
19 B. D. Bath, D. J. Michael, B. J. Trafton, J. D. Joseph, P. L. Runnels and R. M. Wightman, *Anal. Chem.*, 2000, **72**, 5994.
20 D. J. Michael, J. D. Joseph, M. R. Kilpatrick, E. R. Travis and R. M. Wightman, *Anal. Chem.*, 1999, **71**, 3941.
21 E. W. Kristensen, R. L. Wilson and R. M. Wightman, *Anal. Chem.*, 1986, **58**, 986.
22 G. Paxinos and C. Watson, *The Rat Brain in Stereotaxic Coordinates*, Academic Press, San Diego, CA, 1998.
23 P. L. Runnels, J. D. Joseph, M. J. Logman and R. M. Wightman, *Anal. Chem.*, 1999, **71**, 2782.
24 J. X. Feng, M. Brazell, K. Renner, R. Kasser and R. N. Adams, *Anal. Chem.*, 1987, **59**, 1863.
25 B. J. Venton, D. J. Michael and R. M. Wightman, *J. Neurochem.*, 2003, **84**, 373.
26 K. P. Troyer, M. L. Heien, B. J. Venton and R. M. Wightman, *Curr. Opin. Chem. Biol.*, 2002, **6** , 696.
27 B. J. Venton and R. M. Wightman, *Anal. Chem.*, 2003, **75**, 414a.
28 C. J. Fowler, L. Oreland and B. A. Callingham, *J. Pharm. Pharmacol.*, 1981, **33**, 341.
29 M. Holzbauer, K. Racke, S. P. Mann, T. Cooper, G. Cohen, U. Krause and D. F. Sharman, *J. Neural Transm.*, 1984, **59**, 91.
30 A. Colzi, F. D'Agostini, A. M. Cesura, E. Borroni and M. Da Prada, *J. Pharmacol. Exp. Ther.*, 1993, **265**, 103.
31 E. J. Filinger, *Gen. Pharmacol.*, 1994, **25**, 10.